Physica B 404 (2009) 2539–2542

Contents lists available at ScienceDirect

Physica B

journal homepage: www.elsevier.com/locate/physb

Effects of Co doping on antiferromagnetic structure in $CeRhIn_5$

M. Yokoyama [a,*], I. Kawasaki [b], S. Oinuma [b], N. Oyama [a], K. Tenya [c], H. Amitsuka [b]

[a] Faculty of Science, Ibaraki University, Mito 310-8512, Japan
[b] Graduate School of Science, Hokkaido University, Sapporo 060-0810, Japan
[c] Faculty of Education, Shinshu University, Nagano 380-8544, Japan

ARTICLE INFO

PACS:
71.27.+a
74.70.Tx
75.25.+z

Keywords:
Heavy-fermion systems
Antiferromagnetism
Superconductivity
Neutron scattering

ABSTRACT

We performed the elastic neutron scattering experiments on the mixed compounds $CeRh_{1-x}Co_xIn_5$, and found that doping Co into $CeRhIn_5$ dramatically changes the antiferromagnetic (AF) structure. The incommensurate AF state with the propagation vector of $q_h = (\frac{1}{2}, \frac{1}{2}, \sim 0.3)$ observed in pure $CeRhIn_5$ is suppressed with increasing x, and new AF states with an incommensurate $q_1 = (\frac{1}{2}, \frac{1}{2}, \sim 0.4)$ and a commensurate $q_c = (\frac{1}{2}, \frac{1}{2}, \frac{1}{2})$ modulations simultaneously develop near the AF quantum critical point: $x_c \sim 0.8$. These results suggest that the AF correlations with the q_c and q_1 modulations enhanced in the intermediate Co concentrations may play a crucial role in the evolution of the superconductivity observed above $x \sim 0.4$.

1. Introduction

The Ce-based heavy-fermion compounds $CeMIn_5$ (M = Rh and Co: $HoCoGa_5$-type tetragonal structure) are intensively studied for a rich variety of low-temperature properties ascribed to the interplay between antiferromagnetism (AF) and superconductivity (SC). $CeCoIn_5$ shows an unconventional d-wave SC below the transition temperature $T_c = 2.3$ K [1–3]. It is revealed that applying magnetic field breaks the SC state via a first-order phase transition at the upper critical field H_{c2} below 0.7 K, suggesting that the Pauli paramagnetic effect strongly affects the SC state [2,4]. In addition, above H_{c2} the non-Fermi-liquid behavior is observed in the temperature variations of the specific heat and the resistivity, which is considered to be due to a quantum fluctuation induced in the vicinity of an AF quantum critical point (QCP) [5,6]. On the other hand, both the AF and SC phases are observed in $CeRhIn_5$ by tuning pressure p. At $p = 0$ an incommensurate (IC) AF order appears below the Néel temperature $T_N = 3.8$ K, whose structure is proposed to be helical with a propagation vector of $q_h = (\frac{1}{2}, \frac{1}{2}, 0.297)$ [7–9]. The AF phase is weakly suppressed by increasing p, and then the SC order develops above $p = 1-1.5$ GPa [10–13]. It is found that T_c merges with T_N at $p \sim 1.9$ GPa, and the Fermi-surface properties change at $p \sim 2.35$ GPa [14], suggesting an existence of the AF QCP in this p range.

The characteristics of the AF and SC states in the mixed compounds $CeRh_{1-x}Co_xIn_5$ have been investigated by means of specific heat, magnetization, resistivity measurements [15,16]. It is revealed that T_N is reduced with increasing x, and then approaches zero at the QCP: $x_c \sim 0.8$. The SC phase evolves above $x \sim 0.4$, suggesting the coexistence of these two states for $0.4 \leq x \leq 0.8$. Recent elastic neutron scattering (ENS) experiments revealed that a commensurate (C) AF state with the wave vector of $q_c = (\frac{1}{2}, \frac{1}{2}, \frac{1}{2})$ emerges in the intermediate x range [17,18]. This implies that the nature of the magnetic correlation is changed by doping Co, and it may significantly affect the evolution of SC order. It is therefore interesting to investigate the AF structure in the wide x range. In this paper, we report on the ENS experiments for $CeRh_{1-x}Co_xIn_5$ with the entire x range, performed using both the unpolarized and polarized neutron sources.

2. Experiment details

Single crystals of $CeRh_{1-x}Co_xIn_5$ were grown by the In-flux method. To minimize the effect of the neutron absorptions by Rh and In, we prepared the rod-shaped samples along the tetragonal [1 $\bar{1}$ 0] direction (with a typical size of $1.6 \times 1.6 \times 15\ mm^3$) for the neutron scattering experiments. The Co/Rh concentration x and its distribution in the sample were checked by means of the electron probe microanalysis (EPMA) measurements. We used the samples with the homogeneous distribution of x being achieved within a few percent error, and adopt the x values estimated from the EPMA measurements in this study.

The unpolarized ENS experiments for $x = 0.05$, 0.23, 0.43, 0.53, and 0.70 were performed on the triple-axis spectrometers GPTAS (4G) and PONTA (5G) located at the research reactor JRR-3M of the

* Corresponding author. Tel.: +81 29 228 8358; fax: +81 29 228 8403.
E-mail address: makotti@mx.ibaraki.ac.jp (M. Yokoyama).

0921-4526/$ - see front matter © 2009 Elsevier B.V. All rights reserved.
doi:10.1016/j.physb.2009.06.014

JAEA, Tokai. The neutron momentum $k = 3.8\,\mathrm{\AA}^{-1}$ was chosen by pyrographite (PG) monochromator and analyzer, and a combination of $40'-40'-40'-80'$ collimators and two PG filters were used. For the samples with $x = 0.23$ and 0.7, the magnetic field H was applied along the $[1\,\bar{1}\,0]$ direction up to 30 kOe. The polarized ENS experiments for $x = 0.43$ were carried out on the spectrometer PONTA, where we selected the neutron momentum $k = 4.1\,\mathrm{\AA}^{-1}$ with the Heusler monochromator and analyzer, and used the $B-80'-80'-B$ collimators and a PG filter. The spin direction of the incident neutron beam was tuned to be parallel to the scattering vector Q in Helmholtz coils. The polarization ratio of the neutron spins estimated from the weak (110) nuclear Bragg-peak intensity was ~15. Both the measurements were done in the $(h\,h\,l)$ scattering plane and temperature range of $1.4-10$ K using a pumped ^{4}He cryostat.

3. Results and discussion

Fig. 1 shows the unpolarized ENS patterns at 1.5 K for $x = 0.05$, 0.23, 0.43, 0.53, and 0.7 measured at $Q = (\frac{1}{2}, \frac{1}{2}, 1+\zeta)$ $(0 \le \zeta \le 1)$, where instrumental backgrounds were subtracted using the data at 5 K ($>T_N$). A set of satellite Bragg peaks due to the IC-AF order with a modulation of $q_h = (\frac{1}{2}, \frac{1}{2}, \delta)$ was observed at $x = 0.05$ and 0.23. δ are estimated to be 0.295(3) and 0.297(3), respectively, which are the same as the value (0.297) of pure $CeRhIn_5$ [8]. At $x = 0.43$ and 0.53, new Bragg peaks ascribed to the C $q_c = (\frac{1}{2}, \frac{1}{2}, \frac{1}{2})$ structure emerge together with the IC Bragg peaks. In addition, very weak peaks are detected at the Q positions corresponding to a wave vector of $q_1 = (\frac{1}{2}, \frac{1}{2}, \sim 0.4)$, but this order is considered to occur a shorter range along the c-axis for very large widths of these peaks. At $x = 0.7$, the Bragg-peak intensities for the q_c and q_1 structures are enhanced, and simultaneously, the Bragg peaks for the q_h-AF order vanish. The widths of these Bragg peaks seem to approach the resolution limit (about 300 Å in length). The scans at $Q = (0, 0, 1+\zeta)$ $(0 \le \zeta \le 1)$ were also performed for $x = 0.43$ and 0.7 to check the possibility of the other new structures existing, but no additional peak was detected.

To clarify the nature of these new Bragg peaks, we performed the polarized ENS experiments. Displayed in Fig. 2(a) are the ENS patterns in spin-flip and non-spin-flip scattering channels for $x = 0.43$ at 1.4 K, measured at $Q = (\frac{1}{2}, \frac{1}{2}, 1+\zeta)$ $(0.46 \le \zeta \le 0.74)$. Three non-equivalent Bragg peaks are observed at $Q = (\frac{1}{2}, \frac{1}{2}, \frac{3}{2})$, $(\frac{1}{2}, \frac{1}{2}, 1.6)$, and $(\frac{1}{2}, \frac{1}{2}, 1.697)$ in the spin-flip scattering channel, whose positions correspond to the ordering vectors q_c, q_1, and q_h, respectively. On the other hand, no significant reflection is detected in the non-spin-flip scattering channel. In the present experimental geometry on the neutron spins, it is expected that the nuclear scattering is completely non-spin flip, while any magnetic scattering flips the neutron spins. These experimental results thus establish that all of these Bragg peaks originate from the magnetic scattering, i.e., the AF states with the modulations of q_c, q_1, and q_h emerge at $x = 0.43$. It is still unclear in the present study whether these AF states coexist in microscopic scale or not.

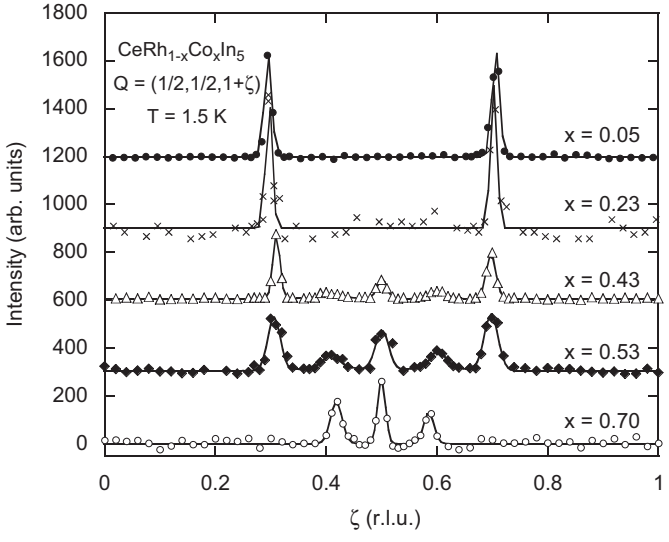

Fig. 1. ENS patterns at 1.5 K for $CeRh_{1-x}Co_xIn_5$ with $x = 0.05$, 0.23, 0.43, 0.53, and 0.7, obtained by scans at $Q = (\frac{1}{2}, \frac{1}{2}, 1+\zeta)$ $(0 \le \zeta \le 1)$ using the unpolarized neutron source. The baselines for the data are shifted for clarity.

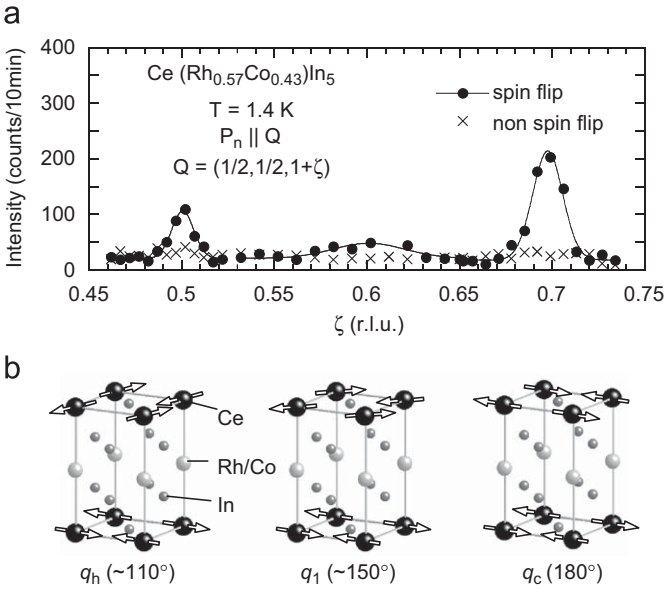

Fig. 2. (a) ENS intensities in spin-flip and non-spin-flip scattering channels at 1.4 K and $Q = (\frac{1}{2}, \frac{1}{2}, 1+\zeta)$ $(0.46 \le \zeta \le 0.74)$ for $CeRh_{0.57}Co_{0.43}In_5$, obtained by the polarized ENS experiments. (b) Arrangements of the magnetic moments on Ce ions for helical (q_h and q_1) and commensurate (q_c) AF structures, depicted in the unit-cell of $CeRh_{1-x}Co_xIn_5$. The angles between nearest-neighbor moments along the c-axis are also shown in (b).

We have estimated the magnetic scattering amplitudes $\mu f(|Q|)$ at 1.5 K for all types of the AF orders at each x from the integrated intensities of the AF Bragg peaks obtained by the longitudinal and transverse scans using unpolarized neutron source. The intensities of the weak nuclear (110) Bragg peaks were used as a reference. We here assume in accordance with the previous reports [8,17,19,20] that both the IC-AF orders have the helical structures, and the moments of all the AF states lie in the tetragonal basal plane [Fig. 2(b)]. The obtained $\mu f(|Q|)$ curves for all the AF states roughly follows the $|Q|$ dependence of the Ce^{3+} magnetic form factor [21], indicating that these AF orders are mainly formed by the Ce 4f moments. In Fig. 3(a) we plot the magnitudes of the AF moments μ_h, μ_1, and μ_c at 1.5 K for the q_h, q_1, and q_c structures, respectively, which are derived from the $\mu f(0)$ values. The μ_h values at $x = 0.05$ and 0.23 are 0.51(5) μ_B/Ce and 0.59(2) μ_B/Ce, respectively, which are close to the values (0.59–0.75 μ_B/Ce) at $x = 0$ [9,22]. With further increasing Co concentration, for $x \ge 0.43$, μ_c and μ_1 develop in connection with the reduction of μ_h. At $x = 0.7$, μ_c and μ_1 reach 0.29(2) and 0.27(2)μ_B/Ce, respectively. The total AF moment defined by the formula